

Jan Zeman; Pavel Gruber

Numerical approach to a rate-independent model of decohesion in laminated composites

In: Jan Chleboun and Petr Přikryl and Karel Segeth and Jakub Šístek (eds.): Programs and Algorithms of Numerical Mathematics, Proceedings of Seminar. Dolní Maxov, June 6-11, 2010. Institute of Mathematics AS CR, Prague, 2010. pp. 239–250.

Persistent URL: <http://dml.cz/dmlcz/702764>

Terms of use:

© Institute of Mathematics AS CR, 2010

Institute of Mathematics of the Czech Academy of Sciences provides access to digitized documents strictly for personal use. Each copy of any part of this document must contain these *Terms of use*.



This document has been digitized, optimized for electronic delivery and stamped with digital signature within the project *DML-CZ: The Czech Digital Mathematics Library*
<http://dml.cz>

NUMERICAL APPROACH TO A RATE-INDEPENDENT MODEL OF DECOHESION IN LAMINATED COMPOSITES*

Jan Zeman, Pavel Gruber

Abstract

In this paper, we present a numerical approach to evolution of decohesion in laminated composites based on incremental variational problems. An energy-based framework is adopted, in which we characterize the system by the stored energy and dissipation functionals quantifying reversible and irreversible processes, respectively. The time-discrete evolution then follows from a solution of incremental minimization problems, which are converted to a fully discrete form by employing the conforming finite element method. Results of a benchmark problem suggest that the resulting model allows to describe both initiation and propagation of interfacial decohesion, with a low sensitivity to spatial discretization.

1 Introduction

The overall behavior of the vast majority of engineering materials and structures is significantly affected or even dominated by the presence of interfaces (i.e. internal boundaries). This is particularly true for composite materials, where interfaces provide weak spots from which damage initiates at different levels of resolution. Therefore, in the engineering community, considerable research efforts have been focused on the adequate description and simulation of interfacial behavior; see, e.g., a recent review [14] for additional details.

During the last decade, the cohesive zone concept has established itself to be a convenient tool to predict interfacial damage initiation and propagation, both from the modeling [19] and computational [3] viewpoints. In this framework, originally introduced for quasi-brittle material by Hillerborg et al. [8], behavior of the bulk material is assumed to be damage-free, whereas the interfacial response is described by means of an inelastic law formulated in terms of interfacial separation and cohesive tractions bridging the crack. Such description is also well-suited to treatment by methods of computational inelasticity, particularly when applied in the *quasi-static setting* (i.e. neglecting viscosity and inertia effects).

Under this modeling assumption, the delamination problem can be conveniently described by the theory of Energetic Rate-Independent Systems developed by Mielke and co-workers, see [11] for a general overview. In this framework, a mechanical system is characterized by a time-dependent *stored energy* functional \mathcal{E} and a *dissipation*

*This work was supported by grant No. 106/08/1379 of the Czech Science Foundation and by the Grant Agency of the Czech Technical University in Prague, grant No. SGS10/020/OHK1/1T/11.

distance \mathcal{D} , quantifying the reversible and irreversible processes in the system, respectively. When supplemented with suitable initial data, evolution of the system then follows from conditions of energetic stability and conservation of energy, formulated solely in terms of \mathcal{E} and \mathcal{D} . This provides a mathematical basis to study a wide range of problems of inelastic solid mechanics in a unified way. Moreover, the framework naturally leads to the *time-incremental energy minimization* concept, thus providing a starting point for the subsequent numerical treatment by optimization methods.

In the context of delamination, the rate-independent approach was first employed by Kočvara et al. [9] to study systems with perfectly brittle interfaces and later extended even to fully rate-dependent systems subject to temperature changes [17]. In this contribution, the focus is on numerical and engineering aspects of the rate-independent setting. In Section 2, we introduce an energy-based delamination model of the Ortiz-Pandolfi type [15], characterized by a piecewise affine traction-separation law. For simplicity, the small-strain setting is adopted and the bulk material is assumed to be described by linear elasticity. In Section 3, we briefly review available existence results for the time-independent problem, which are used to construct fully discrete schemes based on the finite element method in Section 4. The paper is concluded by an illustrative example of flexural delamination.

2 The model setup

Let $\Omega \subset \mathbb{R}^d$ ($d = 2, 3$) be a bounded Lipschitz domain with boundary $\partial\Omega$ and let us consider its decomposition into a finite number of mutually disjoint Lipschitz subdomains $\Omega^{(i)}$, $i = 1, \dots, N$. Further, for $N \geq j > i$, we denote by $\Gamma^{(ij)} = \partial\Omega^{(i)} \cap \partial\Omega^{(j)}$ the (possibly empty) common boundary between $\Omega^{(i)}$ and $\Omega^{(j)}$.

Kinematics of the system is described by independent domain displacement fields $\mathbf{u}^{(i)} : \Omega^{(i)} \rightarrow \mathbb{R}^d$. Local impenetrability is enforced by means of the Signorini condition, requiring

$$\llbracket u_n \rrbracket^{(ij)} \geq 0 \text{ on } \Gamma^{(ij)} \quad \text{where} \quad \llbracket u_n \rrbracket^{(ij)} = \llbracket \mathbf{u} \rrbracket^{(ij)} \cdot \mathbf{n}^{(ij)}, \quad (1)$$

Here, $\mathbf{n}^{(ij)}$ denotes the unit normal to $\Gamma^{(ij)}$ oriented from $\Omega^{(j)}$ to $\Omega^{(i)}$ and $\llbracket \mathbf{u} \rrbracket^{(ij)} = \mathbf{u}^{(i)}|_{\Gamma^{(ij)}} - \mathbf{u}^{(j)}|_{\Gamma^{(ij)}}$, $\llbracket \mathbf{u} \rrbracket^{(ij)} : \Gamma^{(ij)} \rightarrow \mathbb{R}^d$ denotes the interfacial displacement jump, with $\mathbf{u}^{(i)}|_{\Gamma^{(ij)}}$ being the trace of $\mathbf{u}^{(i)}$ on $\Gamma^{(ij)}$. We assume that the system is subject to a time-dependent boundary displacement $\mathbf{w}_D(t)$, $t \in [0; T]$ imposed on the time-independent Dirichlet part of the boundary $\Gamma_D \subset \partial\Omega$. As for the interfacial damage processes, these are quantified by the *damage* variable $\omega^{(ij)} : \Gamma^{(ij)} \rightarrow [0; 1]$, with $\omega^{(ij)}(\mathbf{x}) = 0$ and $\omega^{(ij)}(\mathbf{x}) = 1$ indicating a healthy and a fully damaged interfacial point $\mathbf{x} \in \Gamma^{(ij)}$, see Figure 1(a) for an illustration.

As indicated earlier, we shall characterize evolution of the system by means of certain energetic functionals. First, we introduce the spaces of admissible state variables in the form

$$\mathcal{U} = \left\{ \mathbf{u} \in L^2(\Omega; \mathbb{R}^d) : \mathbf{u}^{(i)} \in W^{1,2}(\Omega^{(i)}; \mathbb{R}^d), \mathbf{u}^{(i)} = \mathbf{0} \text{ on } \partial\Omega^{(i)} \cap \Gamma_D, \right. \\ \left. \llbracket u_n \rrbracket^{(ij)} \geq 0 \text{ on } \Gamma^{(ij)} \right\}, \quad (2)$$

$$\mathcal{Z} = \left\{ \omega \in L^\infty(\cup_{ij} \Gamma^{(ij)}) : \omega^{(ij)} \in L^\infty(\Gamma^{(ij)}) : 0 \leq \omega^{(ij)} \leq 1 \text{ on } \Gamma^{(ij)} \right\}, \quad (3)$$

and define the stored energy functional $\mathcal{E} : [0; T] \times \mathcal{U} \times \mathcal{Z} \rightarrow \mathbb{R}$ as

$$\mathcal{E}(t, \mathbf{u}, \omega) = \sum_{i=1}^N \frac{1}{2} \int_{\Omega_i} \boldsymbol{\varepsilon} \left(\mathbf{u}^{(i)} + \mathbf{u}_D^{(i)}(t) \right) : \mathbf{C}^{(i)} : \boldsymbol{\varepsilon} \left(\mathbf{u}^{(i)} + \mathbf{u}_D^{(i)}(t) \right) d\Omega \\ + \sum_{i=1}^N \sum_{j=i+1}^N \int_{\Gamma^{(ij)}} e^{(ij)} (\llbracket \mathbf{u} \rrbracket^{(ij)}, \omega^{(ij)}) dS, \quad (4)$$

where $\boldsymbol{\varepsilon}(\mathbf{u}) = \frac{1}{2}(\nabla \mathbf{u} + (\nabla \mathbf{u})^\top) \in \mathbb{R}^{d \times d}$ denotes the small-strain tensor, $\mathbf{C}^{(i)} \in \mathbb{R}^{d \times d \times d \times d}$ is the positive-definite material stiffness tensor of the i -th domain and $e^{(ij)} : \mathbb{R}^d \times \mathbb{R} \rightarrow \mathbb{R}$ denotes the density of stored interfacial energy presented later in Section 2.1. Further, $\mathbf{u}_D^{(i)}(t)$ is the restriction of an extension $\mathbf{u}_D(t)$ of the the time-dependent Dirichlet boundary conditions, i.e. $\mathbf{u}_D(t)|_{\Gamma_D} = \mathbf{w}_D(t)$ with $\mathbf{u}_D(t) \in W^{1,2}(\Omega; \mathbb{R}^d)$.

Since the domains are assumed to be elastic, the irreversible processes occur only at the interfaces. Therefore, the dissipation distance $\mathcal{D} : \mathcal{Z} \times \mathcal{Z} \rightarrow \overline{\mathbb{R}}$, quantifying the energy dissipated by changing the internal variable from ω_1 to ω_2 , admits the expression

$$\mathcal{D}(\omega_1, \omega_2) = \sum_{i=1}^N \sum_{j=i+1}^N \int_{\Gamma^{(ij)}} d^{(ij)}(\omega_1^{(ij)}, \omega_2^{(ij)}) dS, \quad (5)$$

where $d^{(ij)} : \mathbb{R} \times \mathbb{R} \rightarrow \overline{\mathbb{R}}$ is the density of dissipated interfacial energy specified next.

2.1 Interfacial constitutive law

To introduce the cohesive zone model, we consider the following decomposition of interfacial displacement jumps (the superscript $\bullet^{(ij)}$ is dropped for the sake of brevity)

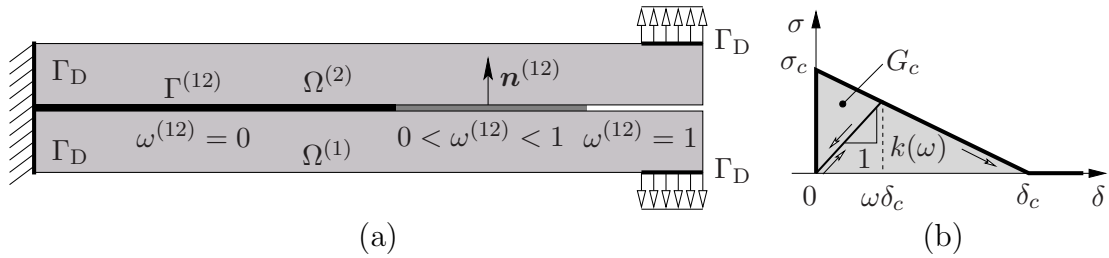


Fig. 1: (a) An example of the introduced notation and of (b) the traction-separation law.

$$[[\mathbf{u}]] = [[u_n]]\mathbf{n} + [[\mathbf{u}_s]], \quad (6)$$

where the normal displacement jump u_n follows from Eq. (1) and $[[\mathbf{u}_s]]$ denotes the tangential component. The vector of interfacial tractions $\mathbf{t} \in \mathbb{R}^d$ is decomposed analogously:

$$\mathbf{t} = \sigma_n \mathbf{n} + \mathbf{t}_s \quad \text{where} \quad \sigma_n = \mathbf{t} \cdot \mathbf{n}. \quad (7)$$

Following [15], we introduce the effective interfacial displacement jumps and tractions in the form

$$\delta([[\mathbf{u}]])^2 = u_n^2 + \beta^2 \| \mathbf{u}_s \|^2, \quad \sigma(\mathbf{t})^2 = \sigma_n^2 + \beta^{-2} \| \mathbf{t}_s \|^2, \quad (8)$$

where $\beta > 0$ is a mode mixity parameter, which needs to be determined from experiments. Due to the adopted linear traction-separation law, the perfect interface (with $\omega = 0$) is characterized by its strength σ_c (in Pa) and maximal effective opening δ_c (in m), cf. Figure 1(b). The area under the traction-separation line gives the density of the dissipated energy $G_c = \frac{1}{2} \sigma_c \delta_c$ for $\omega_1 = 0$ and $\omega_2 = 1$. For general case, this yields the following expression for the stored and dissipated energies:¹

$$e([[\mathbf{u}]], \omega) = \frac{1}{2} \frac{\sigma_c (1 - \omega)}{\delta_c \omega} \delta^2([[\mathbf{u}]]) = \frac{1}{2} k(\omega) \delta^2([[\mathbf{u}]]), \quad (9)$$

$$d(\omega_1, \omega_2) = \begin{cases} G_c(\omega_2 - \omega_1) & \text{for } \omega_2 \geq \omega_1, \\ +\infty & \text{otherwise.} \end{cases} \quad (10)$$

Note that the '+ ∞ ' term in Eq. (10) corresponds to the damage unidirectionality, i.e. the damage variable ω never decreases during the decohesion process.

3 Incremental energetic minimization

The evolution of the mechanical system will be described using a time-incremental approach, where each step corresponds to a variational minimization problem. To this goal, we discretize the time interval $[0; T]$ as $0 = t_0 < t_1 = t_0 + \Delta t < \dots < t_M = T$ and abbreviate $u_k = \mathbf{u}(t_k)$ and $\omega_k = \omega(t_k)$. Then, given the initial condition $(\mathbf{u}_0, \omega_0) \in \mathcal{U} \times \mathcal{Z}$, the time-incremental solution is defined via

Definition 1 (Time-incremental solution). *For $k = 1, 2, \dots, M$, find iteratively $(\mathbf{u}_k, \omega_k) \in \mathcal{U} \times \mathcal{Z}$ such that*

$$(\mathbf{u}_k, \omega_k) = \arg \min_{(\mathbf{u}, \omega) \in \mathcal{U} \times \mathcal{Z}} \mathcal{E}(t_k, \mathbf{u}, \omega) + \mathcal{D}(\omega_{k-1}, \omega). \quad (11)$$

¹Note that for $k \rightarrow \infty$ for $\omega \rightarrow 0_+$, which agrees with the assumption of perfect interface, but leads to numerical difficulties. Therefore, in the numerical experiments, the $\omega = 0$ case is replaced with $\omega = \omega^{\text{in}} < 1$.

The existence of the time-discrete solution to the delamination problem follows from the next proposition, proven in [9]:

Proposition 1. *Assume that $\text{meas}_{d-1}(\partial\Omega^{(i)} \cap \Gamma_D) \neq 0$ for $i = 1, 2, \dots, N$, $\mathbf{w}_D(t_k) \in W^{1/2,2}(\Gamma_D; \mathbb{R}^d)$ for $k = 1, 2, \dots, M$ and that*

$$(\mathbf{u}_0, \omega_0) = \arg \min_{(\mathbf{u}, \omega) \in \mathcal{U} \times \mathcal{Z}} \mathcal{E}(0, \mathbf{u}, \omega) + \mathcal{D}(\omega_0, \omega). \quad (12)$$

Then for all $k = 1, 2, \dots, M$ we have

- i) existence of time-incremental solution $(\mathbf{u}_k, \omega_k) \in \mathcal{U} \times \mathcal{Z}$,
- ii) stability of (\mathbf{u}_k, ω_k) :

$$\mathcal{E}(t_k, \mathbf{u}_k, \omega_k) \leq \mathcal{E}(t_k, \mathbf{u}, \omega) + \mathcal{D}(\omega_k, \omega) \quad (13)$$

for all $(\mathbf{u}, \omega) \in \mathcal{U} \times \mathcal{Z}$,

- iii) two-sided energy inequality

$$\begin{aligned} \int_{t_{k-1}}^{t_k} \partial_t \mathcal{E}(t, \mathbf{u}_k, \omega_k) dt &\leq \mathcal{E}(t_{k-1}, \mathbf{u}_{k-1}, \omega_{k-1}) + \mathcal{D}(\mathbf{u}_{k-1}, \omega_k) - \mathcal{E}(t_k, \mathbf{u}_k, \omega_k) \\ &\leq \int_{t_{k-1}}^{t_k} \partial_t \mathcal{E}(t, \mathbf{u}_{k-1}, \omega_{k-1}) dt. \end{aligned} \quad (14)$$

4 Numerical treatment

The developments presented up to this point provide a convenient framework for an implementable numerical scheme, obtained by discretizing the time-incremental formulation (11) in the space variables by the finite element method. In particular, we employ low-order discretizations of domain displacements $\mathbf{u}^{(i)}$ by P^1 -continuous finite elements and of interfacial damage variables $\omega^{(ij)}$ by P^0 finite elements, as this choice is supported by convergence proofs for $h \rightarrow 0$ in [12].

To this goal, each domain Ω_i is triangulated using elements with a mesh size h . We assume that the discretization is conforming, i.e. that two interfacial nodes belonging to the adjacent domains Ω_i and Ω_j are geometrically identical, and that the same mesh is used to approximate variables \mathbf{u} and ω . Then, the finite element discretization with a suitable numbering of nodes yields a discrete incremental minimization problem in the form

$$\left. \begin{array}{l} \text{minimize} \quad (\mathbf{u}, \mathbf{w}) \mapsto E(t_k, \mathbf{u}, \mathbf{w}) + D(\mathbf{w}_{k-1}, \mathbf{w}) \\ \text{subject to} \quad \mathbf{B}_E \mathbf{u} = \mathbf{0}, \quad \mathbf{B}_I \mathbf{u} \geq \mathbf{0}, \quad \mathbf{w}_{k-1} \leq \mathbf{w} \leq \mathbf{1}. \end{array} \right\} \quad (15)$$

where $\mathbf{u} \in \mathbb{R}^{n_u}$ stores the nodal displacements for individual sub-domains and $\mathbf{w} \in \mathbb{R}^{n_w}$ designates the delamination parameters associated with interfacial element edges. The discretized stored energy functional $E \rightarrow [0; T] \times \mathbb{R}^{n_u} \times \mathbb{R}^{n_w} \rightarrow \mathbb{R}$ receives the form, cf. (4),

$$E(t, \mathbf{u}, \mathbf{w}) = \frac{1}{2} (\mathbf{u} + \mathbf{u}_D(t))^T \mathbf{K} (\mathbf{u} + \mathbf{u}_D(t)) + \frac{1}{2} \llbracket \mathbf{u} \rrbracket^T \mathbf{k}(\mathbf{w}) \llbracket \mathbf{u} \rrbracket, \quad (16)$$

where $\mathbf{K} = \text{diag}(\mathbf{K}^{(1)}, \mathbf{K}^{(2)}, \dots, \mathbf{K}^{(N)})$ is a symmetric positive semi-definite block-diagonal stiffness matrix of order n_u (derived from $\mathbf{C}^{(i)}$), $\llbracket \mathbf{u} \rrbracket \in \mathbb{R}^{n_k}$ stores the displacement jumps at interfacial nodes, and \mathbf{k} is a symmetric positive-definite interfacial stiffness matrix of order n_k , which depends non-linearly on \mathbf{w} as follows from Eq. (9). The discrete dissipation distance is expressed by a linear function

$$D(\mathbf{w}_1, \mathbf{w}_2) = \mathbf{a}^\top (\mathbf{w}_2 - \mathbf{w}_1), \quad (17)$$

where the entries of $\mathbf{a} \in \mathbb{R}^m$ store the amount of energy dissipated by the complete delamination of an interfacial element; see [7, 9] for additional details. The constraints in problem (15) consist of the homogeneous Dirichlet boundary conditions prescribed at nodes specified by a full-rank $m_E \times n_u$ Boolean matrix \mathbf{B}_E , nodal interpenetration conditions specified by a full-rank matrix $\mathbf{B}_I \in \mathbb{R}^{m_I \times n_u}$ storing the corresponding components of the normal vector, and the box constraints on the internal variable.

4.1 Alternating minimization algorithm

<ol style="list-style-type: none"> 1. Require $\mathbf{w}_{(0)}$, set $j = 0$ 2. Repeat <ol style="list-style-type: none"> (a) Set $j = j + 1$ (b) Solve for $\mathbf{u}_{(j)}$: <div style="text-align: right; margin-top: 10px;"> $\left. \begin{array}{l} \text{minimize} \quad \mathbf{u} \mapsto E(t_k, \mathbf{u}, \mathbf{w}_{(j-1)}) \\ \text{subject to} \quad \mathbf{B}_E \mathbf{u} = \mathbf{0} \quad \mathbf{B}_I \mathbf{u} \geq \mathbf{0} \end{array} \right\} \quad (18)$ </div> (c) Solve for $\mathbf{w}_{(j)}$: <div style="text-align: right; margin-top: 10px;"> $\left. \begin{array}{l} \text{minimize} \quad \mathbf{w} \mapsto E(t_k, \mathbf{u}_{(j)}, \mathbf{w}) + D(\mathbf{w}_{k-1}, \mathbf{w}) \\ \text{subject to} \quad \mathbf{w}_{k-1} \leq \mathbf{w} \leq \mathbf{1} \end{array} \right\} \quad (19)$ </div> (d) Until $\ \mathbf{w}_{(j)} - \mathbf{w}_{(j-1)}\ \leq \eta$ 3. Set $\mathbf{u}_k = \mathbf{u}_{(j)}$ and $\mathbf{w}_k = \mathbf{w}_{(j)}$

Tab. 1: Conceptual implementation of the alternating minimization algorithm for the k -th time step and an initial guess $\mathbf{w}_{(0)}$.

The discrete incremental problem (15) represents a large-scale non-convex program (due to the $\mathbf{k}(\mathbf{w})$ -term), which is very difficult to solve using a monolithic approach. Nevertheless, it can be observed that the problem is separately convex with respect to variables \mathbf{u} and \mathbf{w} . This directly suggests the concept of the *alternating minimization algorithm*, proposed by Bourdin et al. [4] for variational models of fracture. In the current context, the algorithm is briefly summarized in Table 1.

The individual sub-problems of the alternating minimization algorithm can be resolved using specialized solvers. In particular, step (18) now becomes a quadratic programming problem, which can be efficiently solved when employing recent developments in duality-based solvers for domains separated by imperfect interfaces [10] and for frictionless contact problems [6]. Owing to the piecewise constant approximation of the delamination parameters, problem (19) can be solved locally element-by-element in a closed form, see [7] for additional details.

4.2 Time-stepping strategy

Even though the alternating minimization algorithm performs well for a wide range of computational examples, it generally converges only to a local minimizer of the objective function (15), which can violate the two-sided energetic inequality (14). Exactly this observation was used in Mielke et al. [13] to propose a heuristic back-tracking strategy summarized for the current problem in Table 2.

<ol style="list-style-type: none"> 1. Set $k = 1$, $\mathbf{w}_0 = \mathbf{w}_{(0)} = \mathbf{0}$ 2. Repeat <ol style="list-style-type: none"> (a) Determine \mathbf{w}_k using the alternating minimization algorithm for time t_k and initial value $\mathbf{w}_{(0)}$ (b) If $\int_{t_{k-1}}^{t_k} \partial_t E(t, \mathbf{u}_k, \mathbf{w}_k) dt \leq E(t_{k-1}, \mathbf{u}_{k-1}, \mathbf{w}_{k-1}) + D(\mathbf{w}_{k-1}, \mathbf{w}_k) - E(t_k, \mathbf{u}_k, \mathbf{w}_k)$ $\leq \int_{t_{k-1}}^{t_k} \partial_t E(t, \mathbf{u}_{k-1}, \mathbf{w}_{k-1}) dt \tag{20}$ <p style="text-align: center;">set $\mathbf{w}_{(0)} = \mathbf{w}_k$ and $k = k + 1$</p> (c) Else set $\mathbf{w}_{(0)} = \mathbf{w}_k$ and $k = k - 1$ (d) Until $k > M$
--

Tab. 2: *Conceptual implementation of time-stepping strategy.*

The computational procedure proceeds as follows. At the k -th time level, the approximate solution is found using the alternate minimization algorithm, initiated with the solution $\mathbf{w}_{(0)}$ (Step 2(a)). If the pair of solutions $(\mathbf{u}_{k-1}, \mathbf{w}_{k-1})$ and $(\mathbf{u}_k, \mathbf{w}_k)$ satisfies the discretized energy inequality, \mathbf{w}_k is certified as an initial guess for the next time level (Steps 2(b)). In the opposite case, the solution $(\mathbf{u}_k, \mathbf{w}_k)$ leads to a smaller value of the objective function (15) at time t_{k-1} than the actual result

$(\mathbf{u}_{k-1}, \mathbf{w}_{k-1})$. Therefore, it is used as an initial guess at time t_{k-1} (Step 2(c));² see also [2] for additional details and further discussion.

It should be emphasized that there is generally no guarantee that the algorithm will locate the global optimum of the objective function (15) for all time levels and that it will converge in a finite number of steps. Computational experiments nevertheless indicate that it is sufficiently robust and that it delivers solutions with (often substantially) lower energies than the basic alternating minimization scheme [2, 5, 13].

5 Example

The basic features of the model will be illustrated by means of the mixed-mode flexure test, adopted from [18]. The beam specimen consists of two non-symmetric aluminum layers, bonded together by a thin layer of resin adhesive. The beam is simply supported and the loading is imposed by a prescribed displacement at the mid-span, increasing linearly with time t up to the final value of 1.5 mm for $t = T = 1$. The delamination is initiated by a pre-existing interfacial crack, see also Fig. 2 for an illustration.

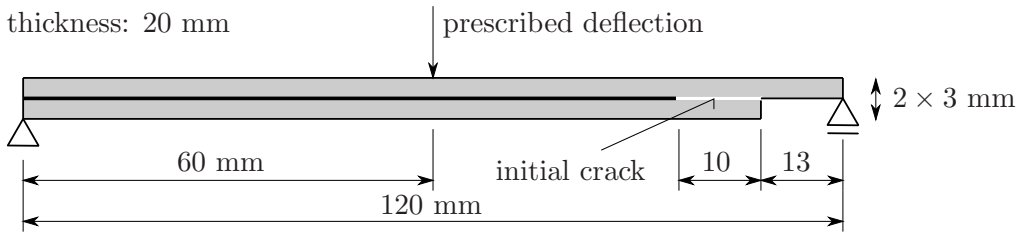


Fig. 2: Setup of the mixed-mode flexure test.

The material properties of the bulk material and the interface appear summarized in Table 3. Two different sets of interfacial properties are considered, one characterized by a higher value of fracture energy G_c and a lower value of initial stiffness $k(\omega^{\text{in}})$ as defined by Eq. (9), whereas the brittle interface corresponds to a low fracture energy G_c and high initial stiffness. The results below correspond to time step $\Delta t = 0.025$ and the value of termination tolerance of the alternating minimization algorithm set to $\eta = 10^{-6}$, recall Table 1. All simulations were performed with an in-house code implemented in MATLAB®.

The energetics of the delamination process for the brittle interface is shown in Figure 3, highlighting the difference between the local energy minimization (full lines) and the time back-tracking scheme (dashed lines). The local scheme predicts initially elastic behavior, followed by complete separation of the two layers at $t \approx 0.56$, resulting in the jump of the dissipated energy $\text{Var}_{\mathcal{D}}$. However, exactly at this step the two-sided inequality is violated, as detected by the back-tracking algorithm. Inductively using such solution as the initial guess of the alternating minimization scheme,

²Note that the stability of initial data (12) ensures that $k \geq 1$.

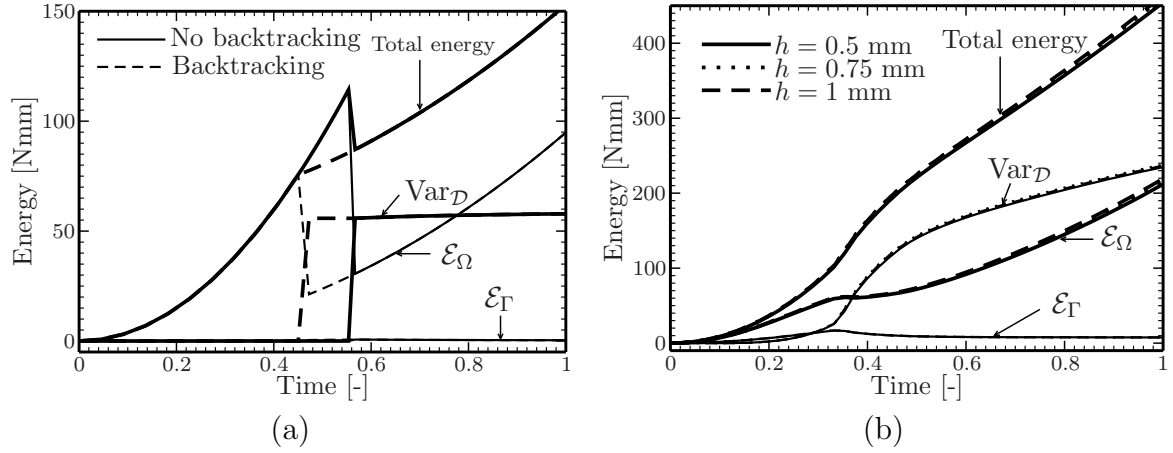


Fig. 3: *Energetics of the delamination process for (a) brittle and (b) ductile interfaces. \mathcal{E}_Ω = energy stored in the bulk, \mathcal{E}_Γ = interfacial stored energy and $\text{Var}_{\mathcal{D}}$ = energy dissipated during the whole process.*

the algorithm returns to the original elastic path, thereby predicting a response leading to a lower value of the total energy for $t \in [0.46, 0.56]$. During the whole time interval, the contribution of the stored interfacial energy \mathcal{E}_Γ remains relatively small, owing to a large value of the interfacial stiffness.

The ductile interface shows a more gradual transition from the elastic response up to the fully debonded state. In this case, the two-sided inequality (20) remains valid during the whole loading program and no back-tracking is necessary. The interfacial delamination initiates first in the shearing mode, which corresponds to a rapid increase in the dissipated energy for $t \in [0.3; 0.4]$. Then it propagates mainly due to opening in the normal direction, which is manifested by the decrease of interfacial energy; see also Fig. 4 for an illustration. We observe that the response remains almost independent on the mesh size h , which is in agreement with theoretical convergence results at disposal. Moreover, no artificial oscillations, reported e.g. in [1], appear in the overall response for both variants of material data. This demonstrates suitability of the algorithm for engineering applications.

Material parameter	Ductile	Brittle
<i>Bulk material</i>		
Young's modulus, E (GPa)	75	75
Poisson's ratio, ν	0.3	0.3
<i>Interface</i>		
Fracture energy, G_c (Jm^{-2})	250	25
Critical stress σ_c (MPa)	5	5
Initial damage ω^{in}	10^{-1}	10^{-3}
Mode mixity parameter β	1	1

Tab. 3: *Material parameters.*

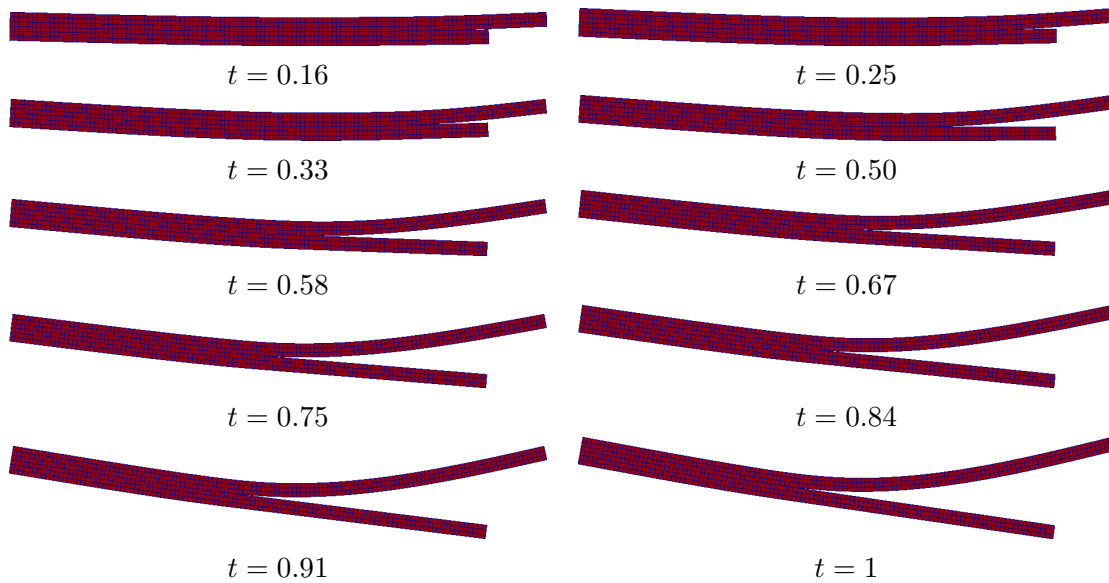


Fig. 4: Snapshots of delamination evolution (displacements depicted as magnified by a factor of 5).

6 Conclusions

In this paper, we have presented a variational model for delamination phenomena based on incremental energy minimization. Its algorithmic treatment relies on the alternating minimization algorithm, complemented with a-posteriori two-sided energy estimates to test the energetic stability of the evolution. Results of the model problem indicate that the method is sufficiently robust for a wide range of material parameters and allows to capture the whole delamination process from the damage initiation up to the complete separation. Note that we have omitted the time-continuous model, obtained as $\Delta t \rightarrow 0$. This aspect, together with additional details and extensions, is available in a recent review [16].

Acknowledgments The authors would like to express their thanks to Martin Kružík, Tomáš Roubíček and Jaroslav Kruiš for numerous discussions on the subject of this work. We also thank an anonymous referee for a number of constructive suggestions which helped us to improve the original version of the paper.

References

- [1] Alfano, G. and Crisfield, M.A.: Finite element interface models for the delamination analysis of laminated composites: mechanical and computational issues. *Int. J. Numer. Methods Eng.* **50** (2001), 1701–1736.

- [2] Benešová, B.: Global optimization numerical strategies for rate-independent processes. *J. Glob. Optim.* (2010). Online First, URL: <http://dx.doi.org/10.1007/s10898-010-9560-6>.
- [3] de Borst, R.: Numerical aspects of cohesive-zone models. *Eng. Fract. Mech.* **70** (2003), 1743–1757.
- [4] Bourdin, B., Francfort, G.A., and Marigo, J.J.: Numerical experiments in revisited brittle fracture. *J. Mech. Phys. Solids* **48** (2000), 797–826.
- [5] Bourdin, B.: Numerical implementation of the variational formulation for quasi-static brittle fracture. *Interface Free Bound.* (2007), 411–430.
- [6] Dostál, Z.: *Optimal Quadratic Programming Algorithms: With Applications to Variational Inequalities, Springer Optimization and Its Applications*, vol. 23. Springer Science+Business Media, New York, NY, 2009.
- [7] Gruber, P., Zeman, J., and Kruis, J.: Numerical modeling of delamination via incremental energy minimization and duality-based solvers, 2010. In preparation.
- [8] Hillerborg, A., Modeer, M., and Petersson, P.: Analysis of crack formation and crack growth in concrete by means of fracture mechanics and finite elements. *Cem. Concr. Res.* **6** (1976), 773–781.
- [9] Kočvara, M., Mielke, A., and Roubíček, T.: A rate-independent approach to the delamination problem. *Math. Mech. Solids* **11** (2006), 423–447.
- [10] Kruis, J. and Bittnar, Z.: Reinforcement-matrix interaction modeled by FETI method. In: *Domain Decomposition Methods in Science and Engineering XVII*, pp. 567–573. Springer Science, 2007.
- [11] Mielke, A.: Evolution in rate-independent systems (Ch. 6). In: C. Dafermos and E. Feireisl (Eds.), *Handbook of Differential Equations, Evolutionary Equations*, vol. 2, pp. 461–559. Elsevier B.V., Amsterdam, 2005.
- [12] Mielke, A. and Roubíček, T.: Numerical approaches to rate-independent processes and applications in inelasticity. *Math. Model. Numer. Anal. (M2AN)* **43** (2009), 399–428.
- [13] Mielke, A., Roubíček, T., and Zeman, J.: Complete damage in elastic and viscoelastic media and its energetics. *Comput. Meth. Appl. Mech. Eng.* **199** (2010), 1242–1253.
- [14] Orifici, A., Herszberg, I., and Thomson, R.: Review of methodologies for composite material modelling incorporating failure. *Compos. Struct.* **86** (2008), 194–210.

- [15] Ortiz, M. and Pandolfi, A.: Finite-deformation irreversible cohesive elements for three-dimensional crack-propagation analysis. *Int. J. Numer. Methods Eng.* **44** (1999), 1267–1282.
- [16] Roubíček, T., Kružík, M., and Zeman, J.: *Delamination and adhesive contact models and their mathematical analysis and numerical treatment*, chap. *Mathematical Methods and Models in Composites*. Imperial College Press, 2010. 45 pages, submitted for publication.
- [17] Roubíček, T. and Rossi, R.: Thermodynamics and analysis of rate-independent adhesive contact at small strains. *Nonlinear Anal.-Theory Methods Appl.* (2010). Submitted for publication, URL: <http://arxiv.org/abs/1004.3764>.
- [18] Valoroso, N. and Champaney, L.: A damage-mechanics-based approach for modelling decohesion in adhesively bonded assemblies. *Eng. Fract. Mech.* **73** (2006), 2774–2801.
- [19] Wisnom, M.R.: Modelling discrete failures in composites with interface elements. *Compos. Pt. A-Appl. Sci. Manuf.* **41** (2010), 795–805.